NAG : 437
pp.1–17 (col.fig.: NIL)
PROD.TYPE: COM
3B2
ED: RM
PAGN: USHAMANI SCAN: AGNES

INTERNATIONAL JOURNAL FOR NUMERICAL AND ANALYTICAL METHODS IN GEOMECHANICS
Int. J. Numer. Anal. Meth. Geomech., 2005; **29**:000–000
Published online in Wiley InterScience (www.interscience.wiley.com). DOI: 10.1002/nag.437

Thermal effects in partially saturated soils: a constitutive model

Gabriella Bolzon[1,*,†] and Bernhard A. Schrefler[2]

[1] *Dipartimento di Ingegneria Strutturale, Politecnico di Milano, 20133 Milano, Italy*
[2] *Dipartimento di Costruzioni e Trasporti, Universitá di Padova, Padova, Italy*

SUMMARY

The present paper is centred on the assessment of an elastic–plastic model for partially saturated soils, earlier proposed by the authors, for its predictive capability with respect to temperature changes, on the light of available experimental results. The model is cast within a constitutive framework that uses Bishop's stress and suction as main variables governing the volumetric response of the material. Some enhancement to the original temperature-independent formulation is proposed. In particular, functions describing the yield surface and the compressibility modulus are modified to account for the shrinking of the elastic domain and for the increase of irreversible volumetric strain with heating. Some examples illustrate the main features of the present proposal. Comparison with some experimental results is also included. Copyright © 2005 John Wiley & Sons, Ltd.

KEY WORDS: porous media; partially saturated soils; constitutive relationships; thermal effects

1. INTRODUCTION

Thermal effects on the consolidation behaviour of saturated clays have been investigated since Campanella and Mitchell [1], who observed that relatively small changes in temperature may cause substantial changes in pore water pressure specially for high effective stress in undrained conditions. They also pointed out that changes in clay structure, due to prevailing physical-chemical phenomena accompanying temperature variations, often consist of swelling during temperature decrease at constant isotropic pressure and compaction during heating, that is just the reverse of what is expected by the expansion/contraction of the soil grains alone.

Consolidation (i.e. irreversible compaction likely associated with local re-arrangements of the material structure) usually occurs in fully saturated normally consolidated soils upon heating. Over-consolidated soils may also exhibit irreversible volumetric strain as temperature raises, in this case mainly expansive, greater than standard thermo-elastic swelling, related to the possibility for macro-pores to expand and to promote particle breakage as a consequence of the fast increase of the pore pressure; usually, this effect increases with the over-consolidation ratio (OCR), see Reference [2] and references therein.

*Correspondence to: Gabriella Bolzon, Dipartimento di Ingegneria Strutturale, Politecnico di Milano, 20133 Milano, Italy.
† E-mail: gabriella.bolzon@polimi.it

Received 6 May 2004
Revised 20 January 2005

The thermal consolidation of fully saturated soils is mainly ascribed to the evolution (shrinking) of the yield surface with temperature. The description of this phenomenon mainly follows the model proposed by Baldi, Hueckel and co-workers [3–6] on the basis of the results of extensive testing carried out on Boom and Pontida clay specimens, results substantially confirmed by recent experimental work; see References [7, 8].

Several improvements to this outstanding reference model have been proposed; for instance: Picard [9] has modified the function which governs thermal effects on consolidation pressure; Robinet *et al*. [2] and Sultan *et al*. [10] have introduced multi-mechanism plasticity to account for the expansive irreversible strains observed for high temperature variation at over-consolidated states; Modaressi and Laloui [11] have considered cyclic plasticity and rate-dependent (visco-plastic) effects.

The consequences of temperature increase on the thermo-mechanical response of partially saturated soils have been investigated in recent years due to their relevance to waste disposal problems. In fact, heating is one main concern of nuclear waste storage but it is promoted also, e.g. by chemical interactions of industrial contaminant losses in wet environment.

Experimental results [12–14] show that the basic behaviour of partially saturated soils is substantially similar at room and at high temperature. Water content at higher temperature is smaller than at room temperature but the effect of heating on water retention curve is almost negligible once normalization has been performed, e.g. with respect to water content at saturation [15].

A controversial aspect is related to the effect of temperature upon compressibility with respect to loading. According to most experimental observations, this parameter is slightly affected by temperature changes, especially in fully saturated or nearly saturated conditions; see, e.g. References [1, 8, 10–13, 16–19]. On the contrary, the experimental results obtained by Romero [14] testing clay samples with different water content and saturation degree, show marked influence of temperature on the virgin consolidation line as suction decreases, i.e. toward fully saturated condition. It is, however, reasonably expected that the structure and sensitivity of different mineral components influence the thermo-mechanical behaviour of soils in different ways [20].

The present paper is centred on the assessment of the elastic–plastic model proposed by Bolzon *et al*. [21] for partially saturated soils, as for its predictive capability with respect to temperature changes, on the light of the above-mentioned published experimental results. Some enhancements are proposed, taking advantage of the hierarchical structure of the original formulation. The resulting constitutive laws can be introduced into general coupled thermo-hydraulical-mechanical frameworks recently put forward, e.g. by Schrefler [22] and Wang and Schrefler [23], or by Thomas *et al*. [24].

The presentation is organized as follows. The original temperature-independent formulation of the considered constitutive model, which uses Bishop's stress [25, 26] and suction as governing variables, is briefly recalled in Section 2. Isotropic materials are considered, so that volumetric and deviatoric behaviour can be uncoupled; no alteration is introduced to the original formulation by Bolzon *et al*. [21] in the deviatoric stress/strain spaces. Temperature effects are introduced first in Section 3, with reference to the fully saturated state, while Section 4 considers the case of partial saturation. A few examples illustrate the model and comparison is made with some available experimental results.

The present proposal is alternative to that by Wu *et al*. [27], which is based on a description of the material behaviour that uses net mean stress instead of Bishop's stress.

2. ELASTO-PLASTIC MODEL FOR PARTIALLY SATURATED SOIL

Following the proposal by Bolzon *et al*. [21], the material model considered herein describes the volumetric behaviour of elastic–plastic partially saturated soils in terms of Bishop's stress [25, 26] and introduces suction as a further stress parameter which controls the evolution of the yield surface and the material hardening.

Bishop's stress can be defined as

$$p' = p - p_a - \chi(p_w - p_a) = \bar{p} + \chi s \tag{1}$$

where p and $\bar{p}$ represent the mean total stress and the commonly used mean total stress in excess of the air pressure (i.e. mean net stress), respectively, while p_w and p_a indicate, respectively, water and air pressure.

In the formulation by Bolzon *et al*. [21], the weighting function χ coincides with relative saturation S_r (i.e. the ratio between water content, w, and water content at full saturation, w_{sat}), which is assumed to be a unique function of suction in the range of interest. Thermo-dynamical considerations support this choice (see, e.g. Reference [28]) although alternative weighting functions χ have been proposed, even in recent literature, to define alternative average skeleton stress, depending also on soil characteristics; see, e.g. References [29–33].

The volumetric behaviour of soil is governed by logarithmic functions of p', depending on the elastic parameter κ and the hardening modulus $H(s) = H_0 H_w(s)$, under the common assumption of additive elastic (superscript e) and plastic (superscript p) strains in the small deformation regime. In particular, in isothermal condition, the reversible strain which develops within the elastic range ($p' < p'_c$, p'_c being the consolidation pressure) or upon unloading ($dp' < 0$) can be evaluated as

$$d\varepsilon_v^e = \frac{\kappa}{v_0} \frac{dp'}{p'} \tag{2}$$

For increasing pressure starting from normally consolidated states ($p' \equiv p'_c$) plastic volumetric strain develops as well, according to the relationship

$$d\varepsilon_v^p = \frac{1}{H_0 H_w(s)} \frac{dp'}{p'} \tag{3}$$

so that

$$d\varepsilon_v = d\varepsilon_v^e + d\varepsilon_v^p = \frac{\lambda(s)}{v_0} \frac{dp'}{p'} \tag{4}$$

In the above formulae: $v_0 = 1 + e_0$ represents the specific soil volume, being e_0 the reference (initial) void radio; $\lambda(s)$ indicates the slope of the virgin consolidation line in the $\varepsilon_v - \ln(p')$ plot; H_0 is the hardening modulus at full saturation, being $H_w(0) = 1$. Clearly,

$$H_0 = \frac{v_0}{\lambda_0 - \kappa}, \quad H_w(s) = \frac{\lambda_0 - \kappa}{\lambda(s) - \kappa} \tag{5}$$

being $\lambda_0 \equiv \lambda(0)$.

In its simplest form, for limited suction range, the dependence on suction of the hardening modulus H_w can be expressed as follows:

$$H_w(s) \equiv 1 + as \tag{6}$$

where the linearization parameter a is related to the material characteristics.

Clearly, more complex relationship can be assumed, depending on available experimental information. For instance, Bolzon *et al.* [21] proposed

$$H_w(s, p') = 1 + (a_1 e^{-p'} - a_2)s \tag{7}$$

or, borrowed from Alonso *et al.* [34]:

$$H_w(s) = [1 + b_1(e^{-b_2 s} - 1)]^{-1} \tag{8}$$

where a_1, a_2, b_1, b_2 are material parameters to be properly calibrated. In what follows, however, we will rest on the simplest assumptions, to outline the essential features of the considered model, to be enhanced for thermal effects.

The current yield surface in the plane p'–s can be obtained through plastic consistency, postulating that p'_c is independent of suction below some threshold value, p'_r; see Reference [34]. The current yield limit p'_{cs} is then related as follows to its corresponding value p'_{c0} in fully saturated condition:

$$p'_{cs}(s) = p'_r \left(\frac{p'_{c0}}{p'_r}\right)^{H_w(s)} \tag{9}$$

3. TEMPERATURE EFFECTS ON FULLY SATURATED SOILS

Bishop's stress (1) reduces to Terzaghi's effective stress when the soil is fully saturated and, therefore, suction reduces to zero. In this particular case, relationship (2) remains unchanged while expression (3) reduces to

$$d\varepsilon_v^p = \frac{1}{H_0}\frac{dp'}{p'} = \frac{\lambda_0 - \kappa}{v_0}\frac{dp'}{p'} \tag{10}$$

where clearly, λ_0 represents the slope of the virgin consolidation line at $s = 0$ and $p' \equiv p'_{c0}$ during plastic flow.

The hardening rule can be obtained by integration of relation (10) during continuous plastic flow, to give

$$p'_{c0}(\varepsilon_v^p) = p'_0 e^{H_0 \varepsilon_v^p} = p'_0 e^{(v_0/\lambda_0 - \kappa)\varepsilon_v^p} \tag{11}$$

where p'_0 represents the initial elastic limit, at reference temperature.

Temperature variations influence the elastic strains which develop at constant effective pressure; this dependence can be analytically described as follows:

$$d\varepsilon_v^e(T) = 3\alpha^e \, dT \tag{12}$$

where α^e represents the isotropic thermal expansion coefficient of the solid skeleton. This coefficient varies with temperature and, slightly, with pressure (see, e.g. References [3, 4, 8]. However, for most applications, α^e can be assumed to be almost constant and relatively small.

Usually $\alpha^{e} \approx 10^{-5 \circ}C^{-1}$: reversible thermal strains (12) are therefore often disregarded, especially when (prevailing) inelastic phenomena take place.

Irreversible volumetric thermal strains are observed upon heating of clay soils, which usually undergo compaction as in standard consolidation test.

Thermal consolidation can be ascribed to a variation of the pre-consolidation pressure, namely to shrinking of the yield surface in the p'–T space, as suggested by Hueckel and Borsetto [5]. This contraction can be described by the following expression, proposed by Picard [9] and experimentally verified by Sultan *et al.* [10]:

$$p'_{cT} = p'_{c0} e^{-\beta^{p} \Delta T} \tag{13}$$

where p'_{cT} represents the consolidation pressure at temperature T, $\Delta T = T - T_0$, T_0 being the reference temperature, β^{p} is a material parameter, possibly depending on T. A good fit of experimental data is usually obtained by assuming

$$\beta^{p} = 3 \frac{1 + e_0}{\lambda_0 - \kappa} \alpha^{p} = 3\alpha^{p} H_0 \tag{14}$$

where the positive scalar (function) α^{p} has the units of a thermal dilatation coefficient, so that $3\alpha^{p}\Delta T$ represents the equivalent unrecoverable volumetric strain.

Relationship (14) is equivalent to that proposed by Modaressi and Laloui [11] when

$$3\alpha^{p} = (a_T \Delta T + b_T)^{-1} \tag{15}$$

A different analytical expression has been considered by Cekerevac and Laloui [8], but the essential features of the above-modelled material response to heating are maintained unaltered.

Combination of (11), (13) and (14) returns

$$p'_{cT}(\varepsilon_{v}^{p}, \Delta T) = p'_{0} e^{H_0(\varepsilon_{v}^{p} - 3\alpha^{p} \Delta T)} \tag{16}$$

ΔT being, in general, the increment with respect to a threshold temperature defined as the highest temperature ever experienced by the soil in its previous deformation history. The influence of temperature on both elastic and post-yield compressibility parameters, (κ and λ_0, and henceforth H_0) is somewhat controversial, but in most materials in saturated or nearly saturated condition, consolidation curves remain substantially parallel at different temperature; see e.g. References [1, 2, 4, 8, 10, 11, 18].

The capability of this model to reproduce the peculiar features of fully saturated soil behaviour under temperature changes is visualized in Figures 1–4.

Figure 1 shows the results of tests performed by Sultan *et al.* [10] on saturated Boom clay, in terms of observed consolidation pressure at different temperature (dots): thermal softening is clearly evidenced. A good fit of these experimental data is represented by the continuous line, obtained from expression (13) for the following set of material parameters: $p'_{c0} = 6$ MPa at the reference temperature $T_0 = 20°C$ (293 K); $\alpha^{p} = 10^{-4}$ K^{-1}. The initial void ratio and compressibility moduli are given by Sultan *et al.* [10]: $e_0 = 0.67$; $\kappa = 0.046$; $\lambda_0 = 0.178$ (henceforth $H_0 = 12.65$).

Figure 2 shows some thermo-mechanical loading paths and the corresponding evolution of the above-defined yield surface (thick line) in the plane p'–T: the initial effective pressure, assumed equal to $p' = 1$ MPa (point A, OCR = 6), is increased first at reference temperature ($T = 20°C$) up to $p' = 5$ MPa (point B, OCR = 1.2) or up to the pre-consolidation value p'_{c0} (point C); the sample is then heated up to different temperatures (20°C, 50°C, 90°C) before the

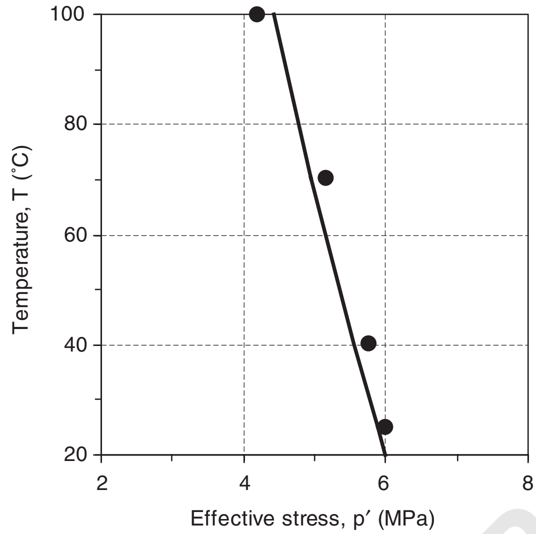

Figure 1. Experimental data in terms of observed consolidation pressure for Boom clay at different temperature (dots) and the corresponding thermal yielding surface according to Sultan *et al*. [10]. Fully saturated condition.

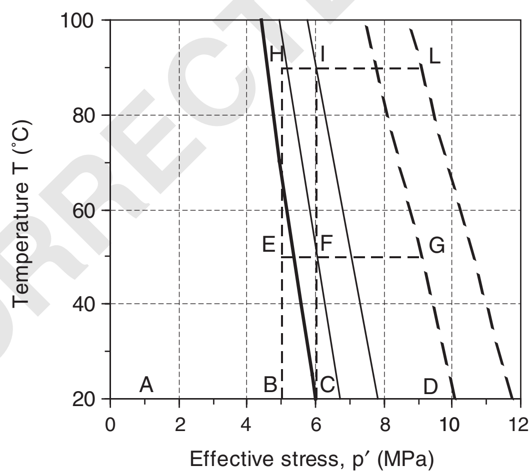

Figure 2. Alternative loading paths and the corresponding evolution of the yield surface in the p'–T plane. Path 1, A → B → C → D: at reference temperature, $T = 20°C$. Path 2(a), A → B → C → F → G: intermediate heating phase up to $T = 50°C$ in normally consolidated condition. Path (2b), A → B → E → F → G: heating up to $T = 50°C$ at over-consolidated state. Path 3(a), A → B → C → F → I → L: heating up to $T = 90°C$ in normally consolidated condition. Path 3(b), A → B → E → H → I → L: heating up to $T = 90°C$ at initially over-consolidated state. Fully saturated condition.

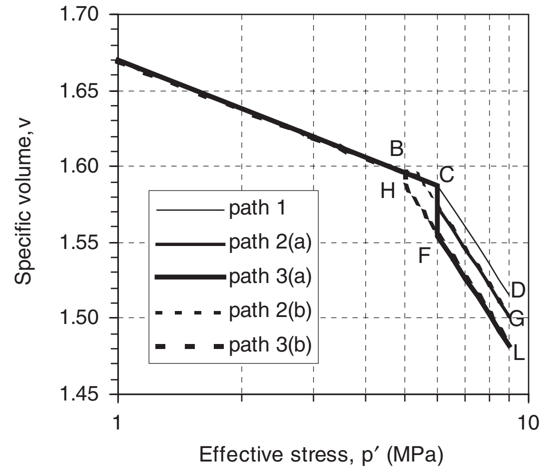

Figure 3. Material response in terms of specific volume versus effective stress along different loading–heating paths. Path 1: at reference temperature, $T = 20°C$. Paths 2(a) and 2(b): heating up to $T = 50°C$. Paths 3(a) and 3(b), heating up to $T = 90°C$. Path details in Figure 2. Fully saturated condition.

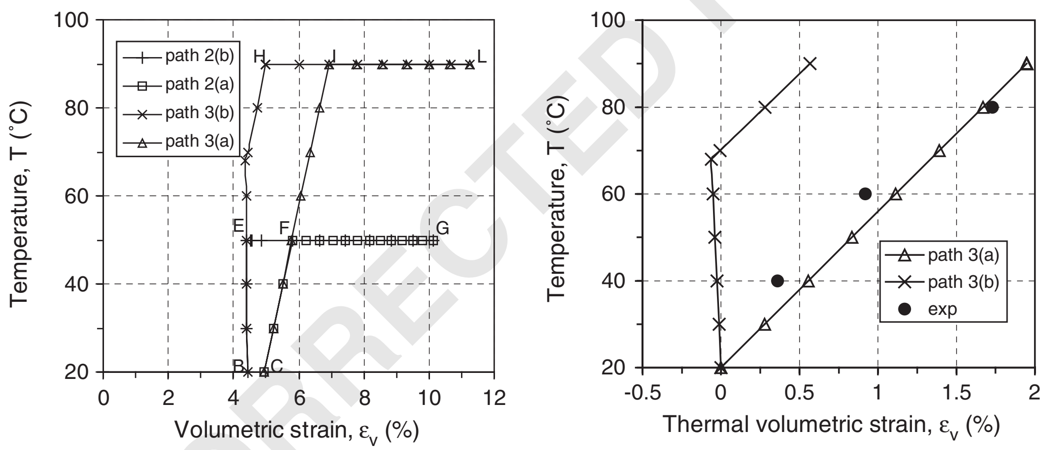

Figure 4. Volumetric strains versus temperature along different loading–heating paths and detail of the volumetric strains developing during heating phases. Circles reproduce the experimental data by Sultan *et al*. [10]. Paths 2(a) and 2(b): heating up to $T = 50°C$ at normally consolidated and over-consolidated states, respectively. Paths 3(a) and 3(b): heating up to $T = 90°C$ at normally consolidated and at initially over-consolidated states. Path details in Figure 2. Fully saturated condition.

final state is reached, characterized by the consolidation pressure $p'_{cT} = 9$ MPa (points D, G or L). Figure 3 shows the material response, as described by the present model, in terms of specific volume versus effective pressure. The expansive and reversible volumetric strains which develop during heating for over-consolidated state and the irreversible compaction exhibited at consolidation are visualized by Figure 4.

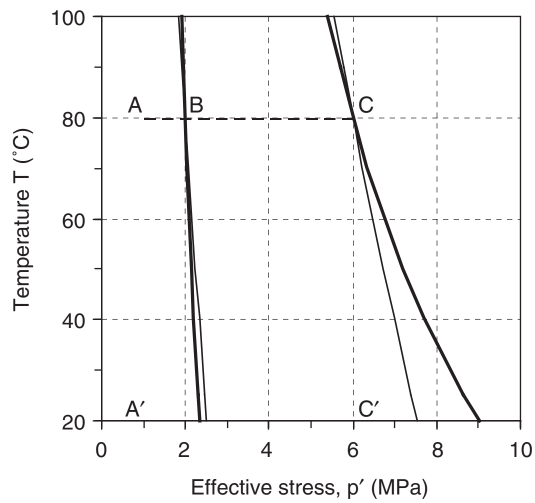

Figure 5. Evolution of the yield surface in the p'–T plane according to different assumptions on the hardening modulus H_0. Thin lines refer to constant H_0; thick lines to H_0 depending on temperature according to (17). Fully saturated condition.

Some clays, tested e.g. by Romero [14] in oedometric conditions at nearly saturated states, show a peculiar behaviour characterized by an increase, with temperature, of both the compression modulus λ and the amount of irreversible volumetric strain which develops for a given effective pressure change under isothermal conditions.

These correlated effects are easily accounted for in the present model, by introducing a suitable dependence of the hardening modulus H_0 on temperature, for instance as follows:

$$H_0(T) = (h_0 + h_T \Delta T)^{-1} \tag{17}$$

Relationship (17) returns the simplest approximation for $\lambda_0(T)$, which thus increases linearly with temperature.

The evolution of the yield surface, and its consequences on the amount of irreversible collapse developed by a material sample loaded at different temperature, are shown by the simulation results drawn in Figures 5 and 6. In this case, for comparison purposes, the material parameters have been calibrated in order to give the same initial yield stress at 80°C; $h_T \approx 1.67 \times 10^{-4}\ \mathrm{K}^{-1}$ has been assumed, consistently with the results published by Romero [14] and by Romero *et al*. [35].

4. TEMPERATURE EFFECTS ON PARTIALLY SATURATED SOILS

Available experimental results show that the behaviour of partially saturated soils is substantially similar at room and at high temperature. Main differences may concern the amount of irreversible volumetric strain which develops upon wetting. Shrinkage upon drying is

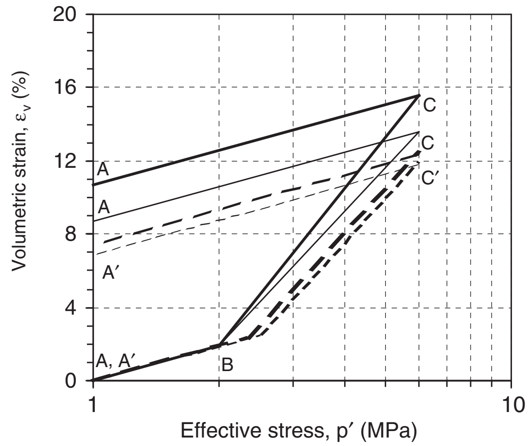

Figure 6. Volumetric strain developing during the loading–unloading paths A → B → C → A at 80°C (continuous lines) and A′ → C′ → A′ at reference temperature (dashed); see Figure 5. Thin lines refer to the elastic–plastic model with constant H_0; thick lines to H_0 depending on temperature according to (17). Fully saturated condition.

also enhanced at high temperature [35] but this aspect is not included in the present model and will not be discussed any further.

Despite the quite limited number of tested sample, results published by Saix and Jouanna [12], Saix [13], Recordon [16], Romero [14] and Romero *et al.* [15, 35] permit to outline the following main features of the thermal behaviour of partially saturated soils:

1. water content at higher temperature is smaller than at reference (room) temperature, but the shape of water retention curve is almost insensitive to heating;
2. suction versus saturation relationship is even less affected by temperature changes;
3. the amount of irreversible strains which develop during wetting may increase with temperature for those soils which exhibit, as peculiar features, irreversible swelling with suction decrease (even at reference temperature) and thermal dependence of the hardening moduli.

In the framework adopted for the present material modelling, relative saturation plays the role of a weighting factor in the stress definition, Equation (1), weight which can be interpreted in the sense of homogenization, for the transition from microscopic to macroscopic material properties; see, e.g. Reference [28].

The water content and the saturation degree of a high-porosity clay material tested by Romero [14] in an extensive experimental campaign are represented in Figure 7: the influence of temperature on the S_r–s relationship is almost negligible.

Data in Figure 7 and similar ones can be interpolated by the analytical expression proposed by van Genuchten [36] and recently modified by Romero *et al.* [15]. Different analytical forms which can be used to this purpose are listed in the review paper by Leong and Rahardjo [37]. Further enhanced expressions have also been proposed, to account for irreversible changes of the saturation degree which might be due, e.g. to hydraulic hysteresis [38, 39]. These non-conventional modelling aspects, however, are not considered in the present work.

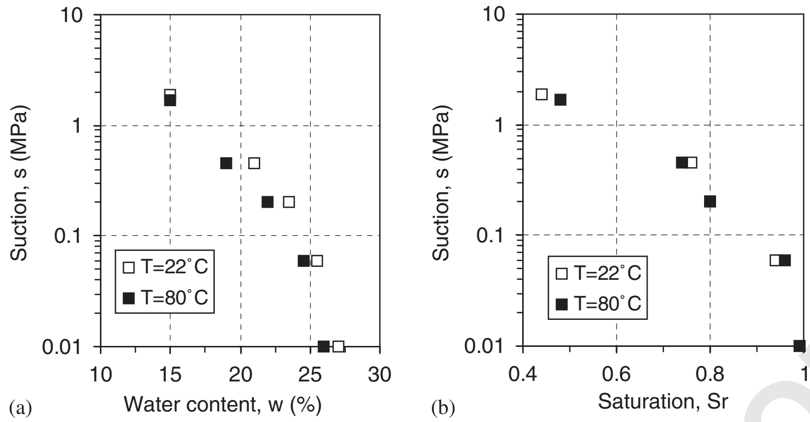

Figure 7. Water content (a) and saturation degree (b) of a high-porosity soil wetted in oedometric condition under constant vertical net stress (0.6 MPa) at different temperature: experimental data by Romero [14].

Partially saturated soils develop unrecoverable volumetric strains with heating in normally consolidated conditions, while thermal strains are reversible in over-consolidated states, exactly as in the case of full saturation. The amount of thermal deformation can be quantified by relationships (12)–(14), the thermal dilatation coefficients α^{e} and α^{p} being again of the order of 10^{-5} and 10^{-4} K, respectively.

As already observed in Section 3, in most instances pre-consolidation stress reduces with heating, while temperature changes do not affect significantly the elastic and plastic material compressibility. Therefore, yield surfaces can be described as follows in the p'–s–T space:

$$p'_{\mathrm{cs}T}(s, \Delta T) = p'_r \left(\frac{p'_{\mathrm{c}T}(\varepsilon_{\mathrm{v}}^{\mathrm{p}}, \Delta T)}{p'_r} \right)^{H_{\mathrm{w}}(s)} \tag{18}$$

the only envisaged change with respect to (9) being the substitution of the consolidation pressure at reference temperature T_0, $p'_{\mathrm{c}0}$, by its corresponding value $p'_{\mathrm{c}T}$ at temperature $T = T_0 + \Delta T$.

Finally, the substitution of expressions (16) and (5) for $p'_{\mathrm{c}T}$ and $H_{\mathrm{w}}(s)$, respectively, returns:

$$p'_{\mathrm{cs}T}(s, \Delta T) = p'_r \left(\frac{p'_0}{p'_r} \right)^{(\lambda_0 - \kappa)/(\lambda(s) - \kappa)} \mathrm{e}^{\frac{v_0}{\lambda(s) - \kappa} (\varepsilon_{\mathrm{v}}^{\mathrm{p}} - 3\alpha^{\mathrm{p}} \Delta T)} \tag{19}$$

Figure 8 shows two sections of the yield surfaces defined by (19) with the above-introduced material parameter set (see Section 3); here, for simplicity, $p'_r = p'_0 = 1$ MPa. The linearization coefficient a (6) has been assumed equal to 0.25 MPa^{-1}.

Figure 9 shows the simulation of the soil response along the two loading, wetting and heating paths also visualized in Figure 8.

A compaction process usually takes place during soil wetting. The corresponding unrecoverable strain can be evaluated through relation (3), being $p' \equiv p'_{\mathrm{cs}T}$, account taken of the fact that plastic compatibility implies the evolution of the consolidation stress with suction

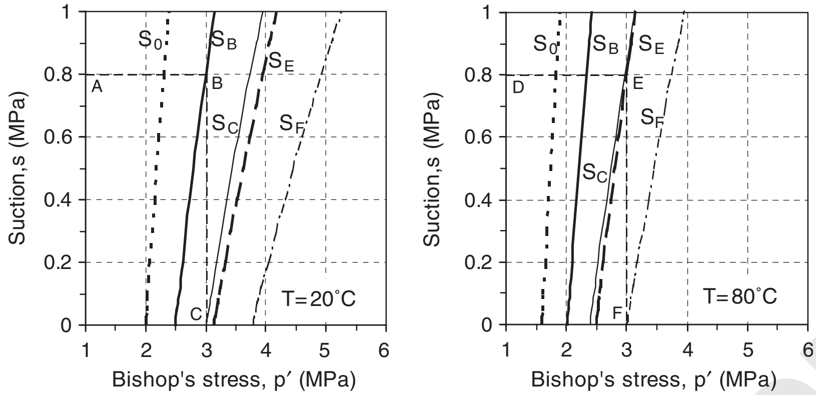

Figure 8. Loading–wetting paths and the corresponding evolution of the yield surface in the p'–s–T space, represented by two sections at $T = 20°C$ (reference temperature) and $T = 80°C$. Path A → B → C: loading up to $p' = 3$ MPa and then wetting at reference temperature ($T = 20°C$). Path D → E → F: loading up to $p' = 3$ MPa and then wetting at high temperature ($T = 80°C$). S_0: initial yield surface, corresponding to the pre-consolidation value $p'_{c0}(s = 0, T = T_0 = 20°C) = 2$ MPa; S_B, S_C, etc.: yield surface at states B, C, etc.

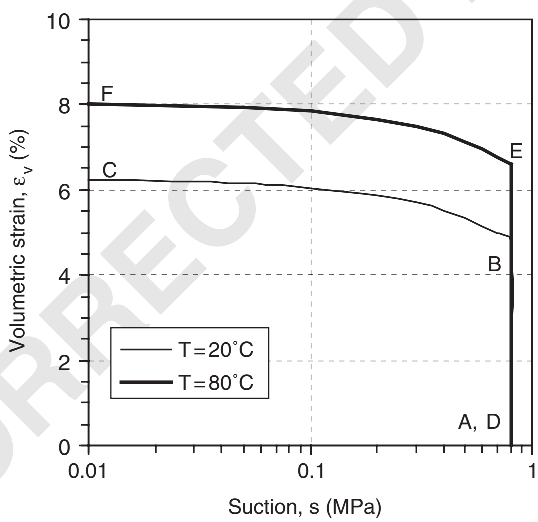

Figure 9. Volumetric strain corresponding to loading–wetting paths at different temperature; see Figure 8.

changes, as schematically shown in Figure 8, path B → C. Notice that the amount of irreversible strain which develops upon wetting is substantially similar at room and high temperature, consistently with the results of some available experimental investigation. In particular, this kind of response has been observed in low density clay at high suction value; see References [14, 35].

A peculiar behaviour is shown by some soils (e.g. low-density clays at low suction values and high-density clays at any suction): irreversible swelling upon wetting occurs even at reference temperature [14, 35]. Contemporarily, increase with temperature both of the slope of the virgin compression line and of the unrecoverable volumetric strain is observed during oedometric tests.

Irreversible swelling can be described by a proper choice of the hardening function; for instance, expression (8) foresees volume increments corresponding to suction reduction for some pressure ranges and suitably chosen parameters a_1, a_2; see the simulations in Bolzon *et al*. [21]. However, the calibration of such a function is beyond the scope of the present investigation, which is focused on thermal effects.

The possible increase of irreversible strain with temperature during the soil wetting is instead easily accounted for even by the simplest version of the present constitutive model, account taken of the contemporarily observed variation of the compressibility modulus.

The curves in Figure 10 shows the function $\lambda(s, T)$ which results from the above assumptions, relations (6) and (17), for the already introduced material parameter values. Clearly, this modification affects the evolution of the consolidation pressure.

Yield surfaces for this case are represented in Figure 11. In particular, the curves indicated by S_E and S_F are relevant to the initial and final state of the soil wetted at high temperature ($T = 80°C$, path E → F). The yield surface sections on the reference temperature ($T = 20°C$) plane are compared with those resulting from the previous simulation (carried out for $\lambda(s)$ independent of T), redrawn from Figure 8. Notice the different relative positions at states E and F, respectively.

Figure 12 compares the soil response to wetting at different temperatures (paths B → C and E → F in Figure 11) in terms of cumulated strains versus suction as simulated by the model, which correctly reproduces the observed trend.

Finally, the model has been used to simulate one of the laboratory tests performed by Romero [14] on a high-porosity clay. In the considered experiment, the soil has been wetted under oedometer conditions at constant vertical net stress 0.6 MPa and at different temperatures, 22 and 80°C. During the test performed at reference temperature (22°C) under controlled suction reduction, both horizontal stress and water content (see Figure 7) have been monitored, besides the volumetric strain. The wetting path undergone by the soil can then be described in terms of suction versus Bishop's stress. Some selected representative points of this

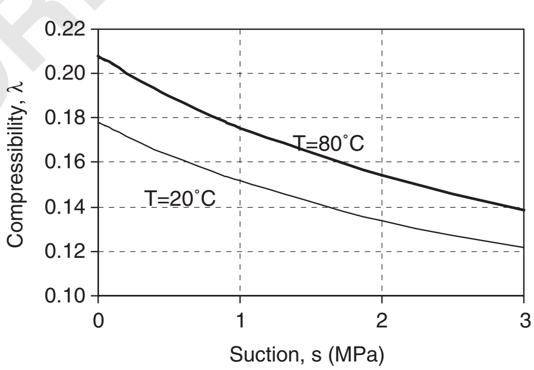

Figure 10. Slope of the virgin consolidation line at reference (thin line) and high (thick line) temperature in partially saturated conditions.

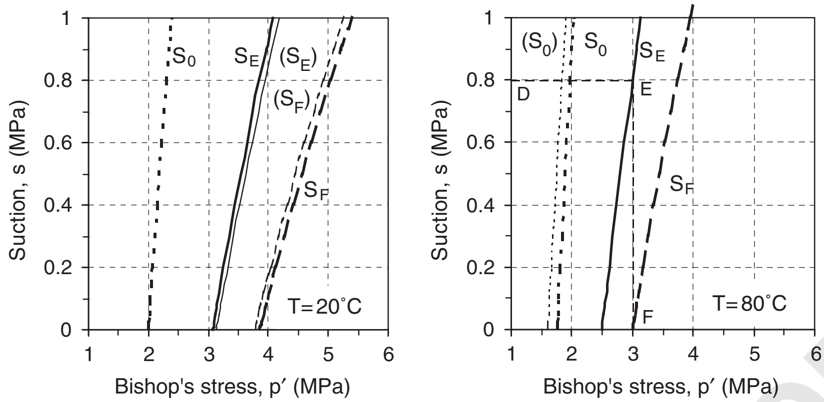

Figure 11. Loading–wetting path at $T = 80°C$ (D → E → F) and corresponding evolution of the yield surface in the p'–s–T space, represented by two sections at $T = 20°C$ (reference temperature) and $T = 80°C$. S_0: initial yield surface at reference temperature, corresponding to the pre-consolidation value $p'_{c0}(s = 0, T = T_0 = 20°C) = 2$ MPa, as in Figure 8; S_E, S_F: yield surface at states E and F; (S_0), (S_E), (S_F): initial yield surface and yield surface at states E and F, redrawn from Figure 8.

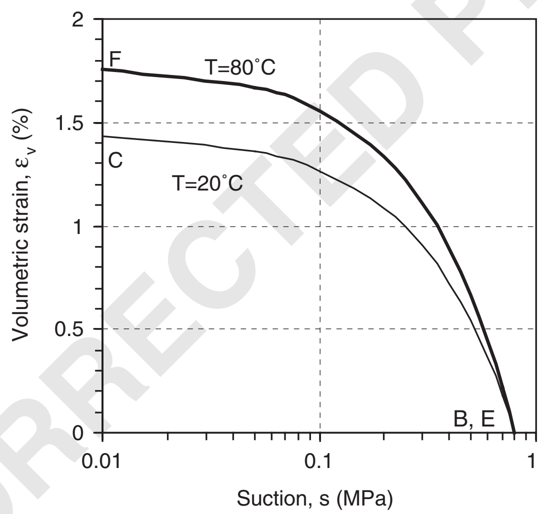

Figure 12. Unrecoverable volumetric strain corresponding to wetting paths (B → C in Figure 9 and E → F in Figure 11) at reference (thin line) and high (thick line) temperature.

path have been linearly interpolated and served as input to the present model simulation; see Figure 12, circles and thick line.

Net mean stress and suction states lying on the same yield surface of this material at reference temperature have been identified by Romero [14] from static compaction and suction controlled tests under isotropic stress. Since suction versus relative saturation relationship is known, this information can be translated into the p'–s plane. Some representative points of this yield limit are plotted in Figure 13 (crosses); the dashed line in the figure represents the linear regression

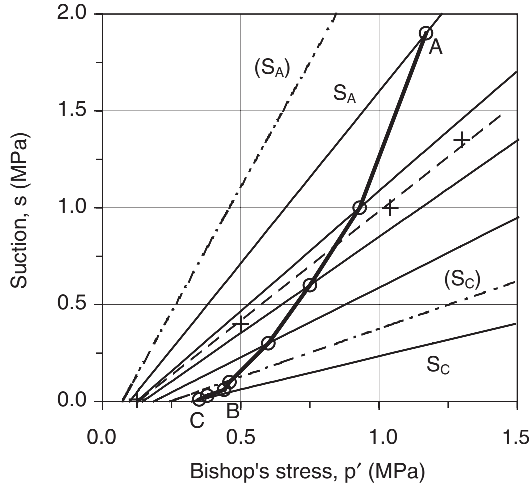

Figure 13. The assumed wetting path (A → B → C) and the corresponding evolution of the yield surface at reference temperature (thin line). Dash–dot lines visualize the trace of S_A and S_C surfaces on the 80°C plane. Crosses represent experimentally determined stress state lying on the same yield locus at reference temperature (22°C); the linear regression curve of these point is also represented (dashed).

curve of these data, with a high correlation factor. This linear interpolation constitutes a reference yield surface in the material model.

An initial void ratio $e_0 = 0.85$ and compressibility moduli $\kappa = 0.01$ and $\lambda_0 = 0.115$ were assumed to characterize the volumetric behaviour of the soil at reference temperature. These values are consistent with the results of oedometric tests performed by Romero [14] at reference temperature, which evidenced elastic and inelastic moduli relating volume changes to vertical stresses in nearly saturated state as high as $\kappa_{\text{oed}}(s \simeq 0) \simeq 0.014$; $\lambda_{\text{oed}}(s \simeq 0) \simeq 0.126$.

The above-selected experimental information and material parameters were used to evaluate the volumetric strains in the soil along the wetting path at reference temperature A → B → C; the obtained results compare satisfactorily with the experiment outcome, see Figure 14.

In the analysis, it was assumed that point A belongs to the initial yield surface, named S_A in Figure 13. The progressive evolution of this locus is also shown in Figure 13 (thin lines); its last configuration is named S_C. The function $\lambda(s)$, see Figure 15, resulted from the consistency condition of plastic deformations. Notice that $\lambda(s = 0.2) \simeq 0.098$, rather close the corresponding experimental value 0.093.

An average 10% increase of $\lambda_{\text{oed}}(s)$ was observed in Romero's experiments heating this soil up to 80°C. Then, it was set $\lambda_0(T = 80°\text{C}) = 0.125$. Further, $\alpha^p = 10^{-4}\ \text{K}^{-1}$ has been chosen, in good accordance with the available laboratory data. The resulting trace of S_A and S_C surfaces on the p'–s plane at 80°C is shown in Figure 13 by dash–dot lines.

The volumetric strains which would develop at 80°C along the wetting path corresponding to A → B → C in Figure 13 are plotted in Figure 14. Comparison with the experimental results is rather good. Notice that this loading condition does not correspond exactly to the laboratory one, since horizontal stresses are expected to change due to the different material compressibility at higher temperature. Nevertheless, a relatively small discrepancy is expected for most part of the experiment. However, the loading step B → C is rather closely aligned with the trace of last

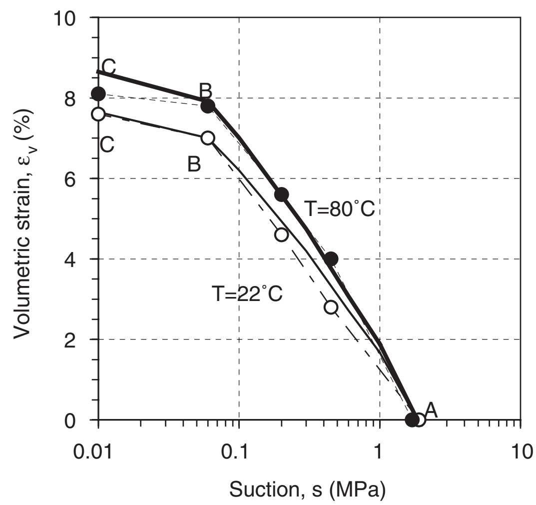

Figure 14. Predicted volumetric strain corresponding to the wetting path A → B → C in Figure 13 at reference (thin line) and high (thick line) temperature. Circles represent experimental data.

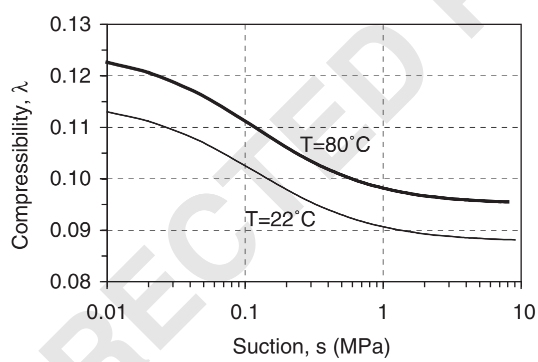

Figure 15. Slope of the virgin consolidation line at reference (thin line) and high (thick line) temperature as defined in the simulation.

yield surface; in this case, small differences in the input data could lead to an elastic solution, with no increase (rather, with a slight decrease) of the volumetric strain, which is also consistent with the experimental observation.

5. CONCLUSION

The elastic–plastic model for partially saturated soils proposed by Bolzon *et al.* (1996) has been considered and its predictive capability with respect to temperature changes has been verified on the light of available experimental results.

It has been shown that the model is fit to the purpose once the functions describing the yield surface and, possibly, the compressibility modulus are modified to account for the shrinking of the elastic domain and for the increase of irreversible volumetric strain with heating.

Further enhancement of the here proposed basic formulation and suitable calibration of the model parameters are the subject of current research. The aim is to return reliable quantitative predictions of partially saturated soil response under complex thermo-mechanical loading.

REFERENCES

1. Campanella RG, Mitchell JK. Influence of temperature variations on soil behaviour. *ASCE Journal of Soils Mechanics and Foundation Division* 1968; **94**(SM3):709–734.
2. Robinet J-C, Rahbaoui A, Plas F, Lebon P. A constitutive thermomechanical model for saturated clays. *Engineering Geology* 1996; **41**:145–169.
3. Baldi G, Hueckel T, Pellegrini R. Thermal volume changes of mineral-water system in low porosity clay soils. *Canadian Geotecnical Journal* 1988; **25**:807–825.
4. Hueckel T, Baldi G. Thermo-plasticity of saturated clays: experimental constitutive study. *ASCE Journal of Geotechnical Engineering* 1990; **116**(12):1778–1796.
5. Huechel T, Borsetto M. Thermo-plasticity of saturated soils and shales: Constitutive equations. *ASCE Journal of Geotechnical Engineering* 1990; **116**(12):1765–1776.
6. del Olmo C, Fioravante V, Gera F, Hueckel T, Mayor JC, Pellegrini R. Thermomechanical properties of deep argillaceous formations. *Engineering Geology* 1996; **41**:87–101.
7. Cekerevac C. Thermal effects on the mechanical behaviour of saturated clays: an experimental and constitutive study. *Doctoral Thesis 2828*, Ecole Polytechnique Fédérale de Lausanne, 2003.
8. Cekerevac C, Laloui L. Experimental study of thermal effects on the mechanical behaviour of a clay. *International Journal for Numerical and Analytical Methods in Geomechanics* 2004; **28**:209–228.
9. Picard J. Ecrouissage thermique des argiles saturées: application au stockage des déchets radioactifs. *Doctoral Thesis*. Ecole Nationale de Ponts ae Chaussées, 1994.
10. Sultan N, Delage P, Cui YJ. Temperature effects on the volume change behaviour of Boom clay. *Engineering Geology* 2002; **64**:135–145.
11. Modaressi H, Laloui L. A thermo-viscoplastic constitutive model for clays. *International Journal for Numerical and Analytical Methods in Geomechanics* 1997; **21**:313–335.
12. Saix C, Jouanna P. Appareil triaxial pour l'étude du comportement thermique de sols non saturés. *Canadian Geotechnical Journal* 1990; **27**:119–128.
13. Saix C. Consolidation thermique par chaleur d'un sol non saturé. *Canadian Geotechnical Journal* 1991; **28**:42–50.
14. Romero E. Characterization and thermo-hydro-mechanical behaviour of unsaturated Boom clay: an experimental study. *Doctoral Thesis*, Universitat Politécnica de Catalunya, 1999.
15. Romero E, Gens A, Lloret A. Temperature effects on the hydraulic behaviour of an unsaturated clay. *Geotechnical and Geological Engineering* 2001; **19**:311–332.
16. Recordon E. Déformabilité des sols non saturés á diverses températures. *Revue Francoise de Géotechnique* 1993; **65**:37–56.
17. Lingnau BE, Graham J, Yarechewski D, Tanaka N, Gray MN. Effects of temperature on strength and compressibility of sand-bentonite buffer. *Engineering Geology* 1996; **41**:103–115.
18. Burghignoli A, Desideri A, Miliziano S. A laboratory study on the thermomechanical behaviour of clayey soils. *Canadian Geotechnical Journal* 2000; **37**:764–780.
19. Delage P, Cui YJ, Sultan N. On the thermal consolidation of Boom clay. *Canadian Geotechnical Journal* 2000; **37**:343–354.
20. Di Maio C, Santoli L, Schiavone P. Volume change behaviour of clays: The influence of mineral composition, pore fluid composition and stress state. *Mechanics of Materials* 2004; **36**:435–451.
21. Bolzon G, Schrefler BA, Zienkiewicz OC. Elastoplastic soil constitutive law generalized to partially saturated states. *Géotechnique* 1996; **46**:279–289.
22. Schrefler BA. Computer modelling in environmental geomechanics. *Computers and Structures* 2001; **79**:2209–2223.
23. Wang Z, Schrefler BA. Fully coupled thermo-hydro-mechanical analysis by an algebraic multigrid method. *Engineering Computations* 2003; **20**:211–229.
24. Thomas HR, Yang HT, He Y, Cleall PJ. A multi-level parallelized substructuring-frontal solution for coupled thermo/hydro/mechanical problems in unsaturated soils. *International Journal for Numerical and Analytical Methods in Geomechanics* 2003; **27**:951–976.
25. Bishop AW. The principle of effective stress. *Teknisk Ukeblad* 1959; **39**:859–863.

26. Bishop AW, Blight GE. Some aspects of effective stress in saturated and partly saturated soils. *Géotechnique* 1963; **13**:177–197.
27. Wu W, Li X, Charlier R, Collin E. A thermo-hydro-mechanical constitutive model and its numerical modelling for unsaturated soils. *Computers and Geotechnics* 2004; **31**:155–167.
28. Gray WG, Schrefler BA. Thermodynamic approach to effective stress in partially saturated porous media. *European Journal of Mechanics – A/Solids* 2001; **20**:521–538.
29. Li X, Zienkiewicz OC. Multiphase flow in deforming porous media and finite elements solutions. *Computers and Structures* 1992; **45**:211–227.
30. Loret B, Kalili N. A three-phase model for unsaturated soils. *International Journal for Numerical and Analytical Methods in Geomechanics* 2000; **24**:893–927.
31. Karube D, Kawai K. The role of pore water in the mechanical behavior of unsaturated soils. *Geotechnical and Geological Engineering* 2001; **19**:211–241.
32. Gallipoli D, Gens A, Sharma R, Vaunat J. An elasto-plastic model for unsaturated soil incorporating the effects of suction and degree of saturation on mechanical behaviour. *Géotechnique* 2003; **53**(1):123–135.
33. Sun DA, Matsuoka H, Cui HB, Xu YF. Three-dimensional elasto-plastic model for unsaturated compacted soils with different initial densities. *International Journal for Numerical and Analytical Methods in Geomechanics* 2003; **27**:1079–1098.
34. Alonso EE, Gens A, Josa A. A constitutive model for partially saturated soils. *Géotechnique* 1990; **40**:405–430.
35. Romero E, Gens A, Lloret A. Suction effects on a compacted clay under non-isothermal conditions. *Géotechnique* 2003; **53**(1):65–81.
36. Van Genuchten MT. A closed-form equation for predicting the hydraulic conductivity of unsaturated soils. *Soil Science Society of America Journal* 1980; **44**:892–898.
37. Leong EC, Rahardjo H. Review of soil-water characteristic curve equations. *ASCE Journal of Geotechnical and Geoenvironmental Engineering* 1997; **123**(12):1106–1117.
38. Tinjum JM, Benson CH, Blotz LR. Soil water characteristic curves for compacted clays. *ASCE Journal of Geotechnical and Geoenvironmental Engineering* 1997; **123**(11):1060–1069.
39. Gallipoli D, Wheeler SJ, Karstunen M. Modelling the variation of degree of saturation in a deformable unsaturated soil. *Géotechnique* 2003; **53**(1):105–122.

